Carbohydrate Polymers 180 (2018) 297–303

Contents lists available at ScienceDirect

Carbohydrate Polymers

journal homepage: www.elsevier.com/locate/carbpol

Physicochemical study of ascorbic acid 2-glucoside loaded hyaluronic acid dissolving microneedles irradiated by electron beam and gamma ray

Suyong Kim[a,b], Jeongwon Lee[a], F. Lahiji Shayan[a], Seohyun Kim[b], Inyoung Huh[a], Yonghao Ma[a], Huisuk Yang[a], Geonwoo Kang[a], Hyungil Jung[a,b,*]

[a] Department of Biotechnology, Yonsei University, 50 Yonsei-ro, Seodaemun-gu, Seoul 03722, Republic of Korea
[b] Juvic Inc., Yonsei Engineering Research Park, 50 Yonsei-ro, Seodaemun-gu, Seoul 03722, Republic of Korea

ARTICLE INFO

Keywords:
Dissolving microneedle
Ascorbic acid 2-glucoside
Hyaluronic acid
Terminal sterilization
Electron beam
Gamma ray

ABSTRACT

A dissolving microneedle (DMN) patch encapsulated with ascorbic acid 2-glucoside (AA2G) in a needle-shaped hyaluronic acid (HA) backbone was fabricated and sterilized by electron beam (e-beam, 5–40 kGy) and gamma ray (γ-ray, 5–30 kGy). DMN structures maintained their morphologies and fracture force regardless of e-beam and γ-ray irradiation doses. Both e-beam (40 kGy) and γ-ray (20 and 30 kGy) met the product sterility requirements for cosmetics and vaccines; however, γ-ray irradiation significantly degraded the encapsulated AA2G, while e-beam maintained AA2G activity. Thus, an e-beam dose of 40 kGy, which satisfied the sterility requirements without loss of AA2G, is suitable for terminal sterilization of DMNs. Moreover, we confirmed that the optimized irradiation (e-beam, 40 kGy) did not affect dissolution rate and drug release profile of DMNs. Further, we confirmed that HA, the backbone polymer of DMNs, could be utilized as a stabilizer that inhibits degradation of encapsulated AA2G by irradiation. This detailed analysis can be developed further to optimize various biological drugs in transdermal drug delivery systems.

1. Introduction

Drugs such as biotherapeutics or vaccines are typically administered by injection, which is a low-cost, rapid, and direct way to deliver almost any type of molecule. However, hypodermic needles cannot easily be used by patients at home, and can cause various side effects such as skin irritation, pain, and local injury, leading to discomfort (Giudice & Campbell, 2006; Rogers, 2010). Although oral delivery usually prevents these problems, many drugs cannot be administered orally because of low absorption rates and drug degradation in the gastrointestinal tract (Rowland, 1972; Singh, Singh, & Lillard, 2008). To overcome these limitations, numerous transdermal drug-delivery systems have been developed, combining enhanced efficacy with patient-friendly delivery (Anirudhan, Nair, & Nair, 2016; Kong & Park, 2011; Kong, Kim, & Park, 2016; Prausnitz & Langer, 2008).

Dissolving microneedles (DMNs) have been conceptualized and developed as one such drug-delivery system (Kim, Park, & Prausnitz, 2012; Park, Allen, & Prausnitz, 2005; Tadwee, Gore, & Giradkar, 2011). Drugs are encapsulated in a needle-shaped biodegradable polymer matrix and released directly into the dermal layers as the polymer needles penetrate the skin; this method enhances drug delivery while improving patient compliance and safety (Chu, Choi, & Prausnitz, 2010; Kim, Kim, Yang, Lee, & Jung, 2013; Kim et al., 2016; Mistilis, Bommarius, & Prausnitz, 2015). However, as DMNs pierce the skin and contact tissues directly, the final product must meet stringent standards of sterilization for application in patients. A failure of product sterility could lead to an infection from microorganisms, and such a product should not be released in the market (Tidswell, 2011). To meet standards of product sterility, either terminal sterilization or manufacture via aseptic processing is necessary. Terminal sterilization is the process whereby a product is sterilized in its final packaging, while the aseptic processing sterilizes individual products separately and assembles in a sterile environment. However, aseptic manufacturing can raise the production cost and only be used when terminal sterilization is inapplicable (U.S. Food and Drug Administration, 2004). Therefore, the terminal sterilization process is the most important step in eliminating microorganisms economically and effectively.

Depending on the purpose of sterilization and the material to be sterilized, various terminal sterilization methods have been developed, including dry-heat sterilization, pressured-vapor sterilization, chemical sterilization (with ethylene, formaldehyde, or peracetic acid), and radiation sterilization (electron beam [e-beam] and gamma ray [γ-ray]) (Asasutjarit et al., 2017; Marreco, Moreira, Genari, & Moraes, 2004; Silindir & Ozer, 2009). However, as DMNs are composed of biopolymers

* Corresponding author at: Department of Biotechnology, Yonsei University, 50 Yonsei-ro, Seodaemun-gu, Seoul 03722, Republic of Korea.
E-mail address: hijung@yonsei.ac.kr (H. Jung).

http://dx.doi.org/10.1016/j.carbpol.2017.10.044
Received 21 June 2017; Received in revised form 26 September 2017; Accepted 11 October 2017
Available online 13 October 2017

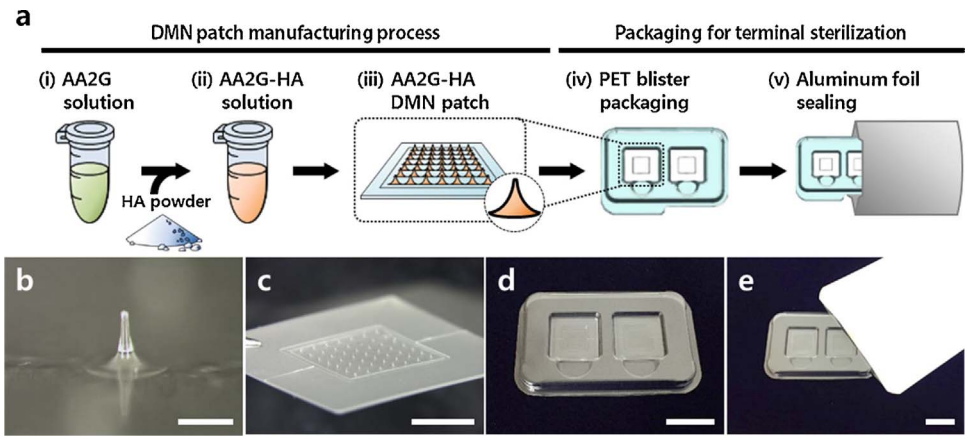

Fig. 1. (a) Schematic illustration of overall ascorbic acid 2-glucoside (AA2G)-hyaluronic acid (HA) dissolving microneedle (DMN) patch manufacturing process; (i) AA2G solution, (ii) AA2G-HA solution, (iii) AA2G-HA DMN patch, (iv) PET blister packaging, and (v) aluminum foil-wrapper sealing. (b) Single DMN (scale bar, 300 μm) and (c) whole DMN patch image (scale bar, 5 mm). (d) The patches were placed in PET blister packs (thickness: 280 μm; scale bar, 20 mm), and (e) the blister packs were sealed in aluminum foil wrappers (thickness: 100 μm; scale bar, 200 mm).

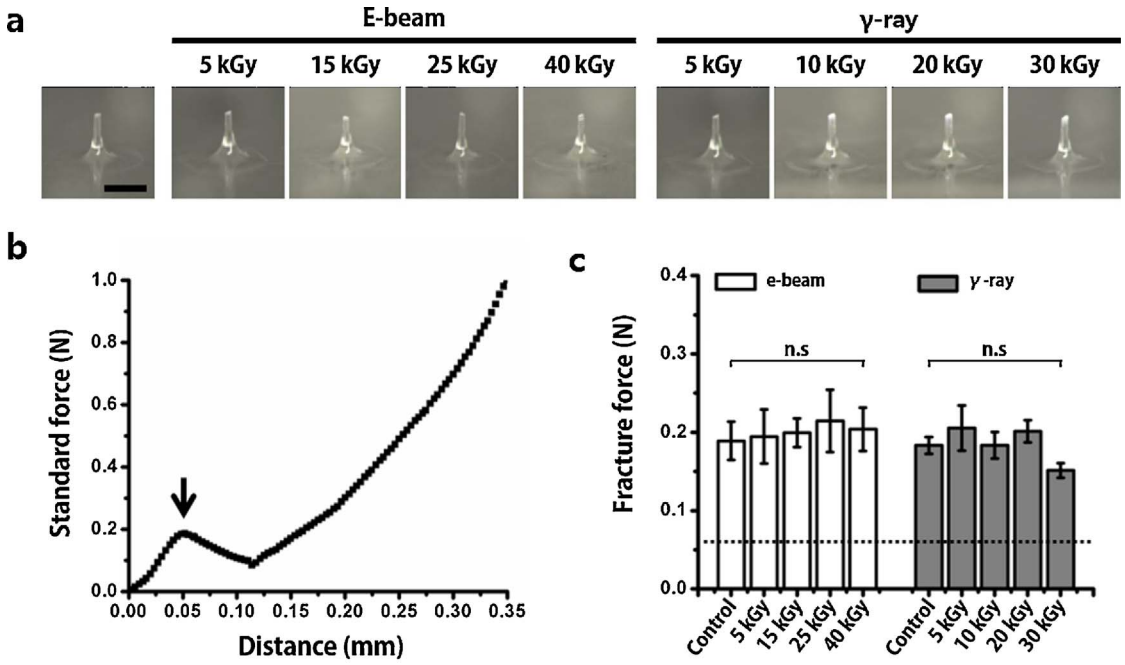

Fig. 2. Microscopic images and fracture force analysis of terminal-sterilized ascorbic acid 2-glucoside (AA2G)-hyaluronic acid (HA) dissolving microneedle (DMN) structures. (a) No morphological changes were observed regardless of e-beam and γ-ray irradiation dose (scale bar, 300 μm). (b) Standard force of a single DMN in the control group, recorded by moving the probe as the axial of distance; the peak of the graph indicates the fracture force of a single DMN (arrow). (c) Neither e-beam nor γ-ray irradiation affected the strength of the DMN structures (n = 4, mean ± SEM). The dashed line represents the minimum fracture force of a single DMN required for skin penetration (0.058 N).

Table 1
Effects of e-beam and γ-ray irradiation on microbial contamination levels of packaged ascorbic acid 2-glucoside (AA2G)-hyaluronic acid (HA) dissolving microneedle (DMN) patches. AA2G-HA DMN patches were dissolved in 50.0 mL of distilled water and evaluated for total aerobic bacterial viable count, total aerobic yeasts and molds viable count, and the presence of *Escherichia coli*, *Pseudomonas aeruginosa*, and *Staphylococcus aureus*.

Test item	Control	e-beam (kGy)				γ-ray (kGy)			
		5	15	25	40	5	10	20	30
Total aerobic viable count (bacteria)	< 10 CFU/mL	< 10 CFU/mL				< 10 CFU/mL			
Total aerobic viable count (yeasts and molds)	< 10 CFU/mL	< 10 CFU/mL				< 10 CFU/mL			
Escherichia coli	None	None				None			
Pseudomonas aeruginosa	None	None				None			
Staphylococcus aureus	None	None				None			

and encapsulated drugs, harsh conditions during the terminal sterilization process, such as heat, moisture, and chemical exposures, can deform DMN morphology and degrade the encapsulated drug, resulting in the failure of DMN functions. Therefore, radiation sterilization, which destroys microorganisms without heat, moisture, or chemicals, is expected to be suitable for DMN product sterilization. However, high-energy transfer from the e-beam and γ-ray irradiations may degrade DMN morphologies or the drug inside the polymer matrix by chemical attacks of free radicals or reactive oxygen species, which can cause dramatically reduced efficacy or induce unexpected side effects (Ameri, Wang, & Maa, 2010; Grieb et al., 2002). Moreover, the degree of this degradation may differ between e-beam and γ-ray irradiations, since γ-ray exhibits higher penetration into sterilizing materials at lower doses than e-beam (Woo & Sandford, 2002). Therefore, selection of an appropriate irradiation method and doses that minimize activity loss of the drug in the DMNs while satisfying standards of sterility is required. To the best of our knowledge, however, an in-depth analysis of these radiation sterilization methods for DMNs has not been reported yet.

In this study, DMN patches composed of hyaluronic acid (HA, with average molecular weight of 39 kDa) and ascorbic acid 2-glucoside

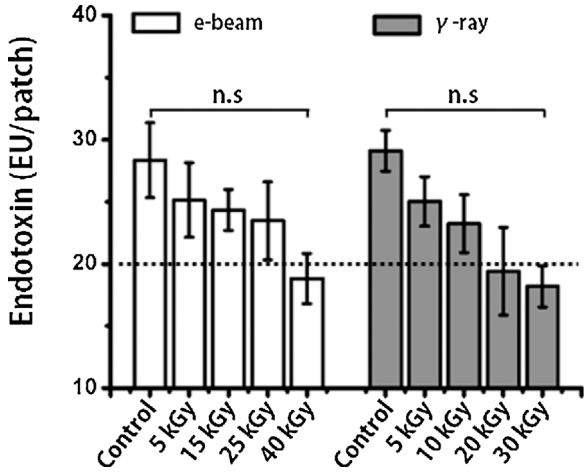

Fig. 3. Effects of e-beam and γ-ray irradiations to endotoxin levels in packaged ascorbic acid 2-glucoside (AA2G)-hyaluronic acid (HA) dissolving microneedle (DMN) patches. Both e-beam and γ-ray irradiations reduced endotoxin levels (n = 4, mean ± SEM). The dashed line represents the endotoxin limit of medical devices for vaccination (20 EU).

(AA2G) were fabricated and sterilized by e-beam and ɣ-ray with irradiation doses of 5–40 kGy and 5–30 kGy, respectively. HA was selected as the DMN backbone material because it is known as a safe and biodegradable polymer approved for use in transdermal drug delivery (Becker et al., 2009). AA2G, which is a vitamin C derivative and widely used in cosmetics, was selected as a model drug because it was expected to be oxidized easily by the radicals generated from irradiation (Chandrasekharan, Kagiya, & Nair, 2009; Girennavar et al., 2008; Mathew et al., 2007; Wong & Kitts, 2001). After the irradiations, we confirmed the skin-penetration function of AA2G loaded HA DMN patches (AA2G-HA DMN patch) by morphological and fracture force analysis. In addition, AA2G-HA DMN patch sterility was assessed by analyzing microbial contamination and endotoxin contamination levels. Moreover, quantitative analysis and free-radical scavenging activity were investigated to evaluate the antioxidant activity of AA2G-HA DMN patch. Further, dissolution rate and release profile of AA2G-HA DMN patch were compared to confirm the effect of irradiation. Finally, we analyzed the antioxidant effect of HA on AA2G activity to investigate drug-polymer interactions. This detailed analysis offers a way to satisfy the sterility requirements without activity loss of encapsulated cosmeceutical and pharmaceutical drugs in multiple biodegradable polymer matrices.

2. Material and methods

2.1. Materials

AA2G was purchased from Hayashibara Corporation (Okayama, Japan). HA (average molecular weight of 39 kDa, PrimalHyal50) was purchased from Soliance (Pomacle, France). Sterile 2.0-mL microtubes were purchased from Axygen Inc. (Union City, CA, USA). Trifluoroacetic acid (TFA) and acetonitrile for high-performance liquid chromatography (HPLC), 2,2-diphenyl-1-picrylhydrazyl (DPPH), and ethanol for the DPPH assay were purchased from Sigma-Aldrich (St. Louis, MO, USA). Limulus amebocyte lysate kit (QCL-1000™) was purchased from Lonza (Basel, Switzerland). Sterile 96-well test plates were purchased from TPP® (Trasadingen, Switzerland). Hair-less pig cadaver skin (thickness: 1 mm) was purchased from Cronex (Hwaseong, Korea). Phosphate-buffered saline (10 mM, pH 7.4) was purchased from Life Technologies (Carlsbad, CA, USA).

2.2. Sample preparation and microscopic imaging

For the AA2G solution, 2.0% (w/v) AA2G powder was dissolved in distilled water and immediately vortexed for 10 s. Next, 65.0% (w/v) HA powder was added to the solution and homogenized at 5000 rpm for 10 min in a planetary centrifugal mixer (ARV-310; Thinky Corp., Tokyo, Japan). Using this solution, 13-μg AA2G-HA DMN patches were fabricated into 7 × 7 arrays by centrifugal lithography (Yang et al., 2017) on a sticky gel-foam sheet after plasma treatment (PDC-32G, Harrick Plasma, Ithaca, NY, USA). For final packaging, two AA2G-HA DMN patches were placed in a polyethylene terephthalate (PET) blister pack (thickness: 280 μm); the blister pack was sealed in an aluminum foil wrapper (thickness: 100 μm). In addition, 1 mL each of AA2G solution and AA2G-HA solution and a AA2G-HA DMN patch were prepared in sterile 2.0-mL microtubes. All samples were prepared non-aseptically to evaluate sterility levels following the sterilization methods. Images of the terminal sterilized DMN patch and dissolved DMN structures applied on a pig cadaver skin at 0, 5, 10 and 20 min were visualized using a bright field microscope (M165FC, Leica, Wetzlar, Germany) to observe morphological changes and dissolution rate, respectively.

2.3. E-beam and γ-ray irradiation

E-beam irradiation was conducted by Seoul Radiology Services (Seoul, Korea) using an 8-kW high-energy linear accelerator (10 MeV, MB10-8/635, Mevex Corp., Stittsville, ON, Canada) at 5, 15, 25, and

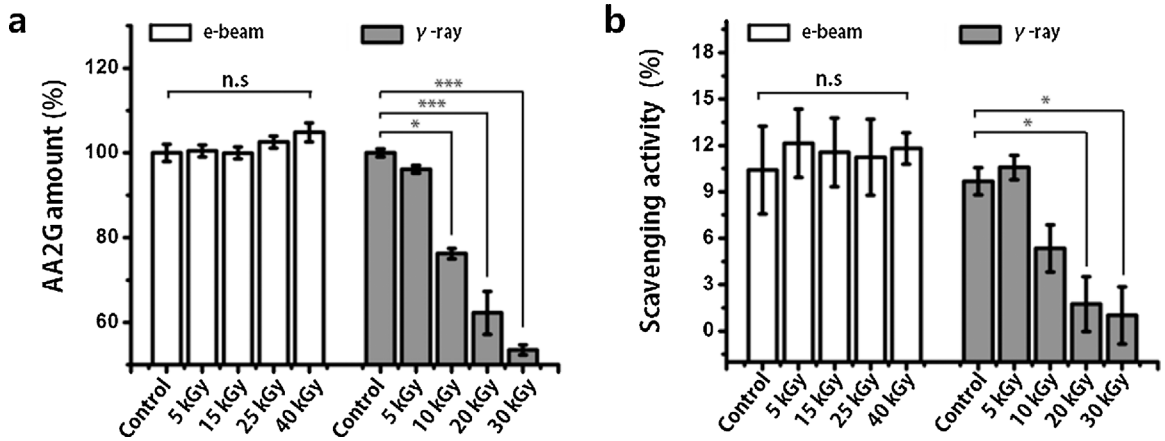

Fig. 4. Quantitative analysis and free-radical scavenging activity of packaged ascorbic acid 2-glucoside (AA2G)-hyaluronic acid (HA) dissolving microneedle (DMN) patches. (a) AA2G content decreased significantly only in the γ-ray-irradiated group; there were no changes in the e-beam-irradiated group (n = 4, mean ± SEM, $^{*}p < 0.05$, $^{***}p < 0.001$). (b) Similarly, the radical-scavenging activity decreased significantly only in the γ-ray-irradiated group, indicating that γ-rays penetrated the packaging and degraded the encapsulated AA2G, while e-beam irradiation did not (n = 4, mean ± SEM, $^{*}p < 0.05$).

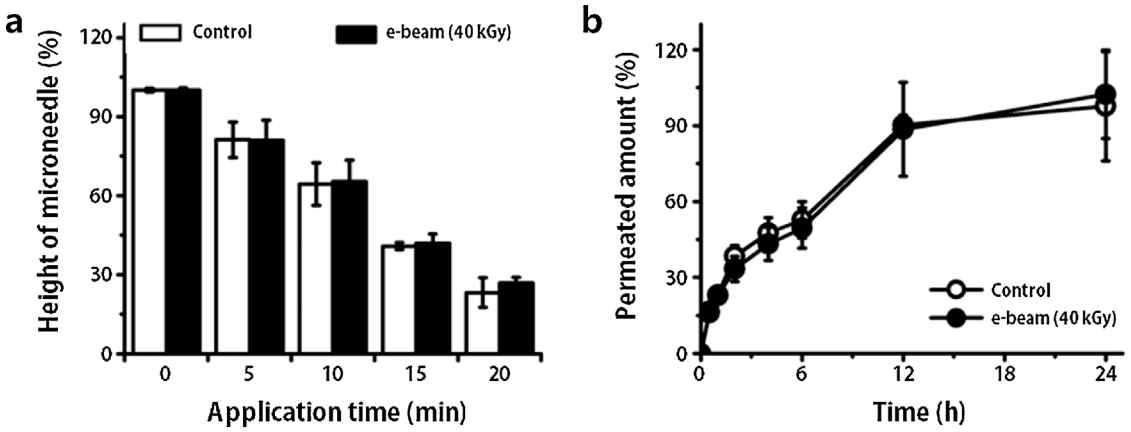

Fig. 5. Comparison of dissolution rate and *in vitro* permeation studies between non-irradiated group (control) and e-beam-irradiated group (40 kGy). (a) DMN structures were gradually dissolved inside the skin over time after application of a DMN patch and a decrease of the height of microneedle between two groups were not significantly different (n = 4). (b) Similarly, the permeated amount of AA2G using a Franz diffusion cell showed similar release profile over 24 h without any significant differences between two groups (n = 4).

40 kGy. ɣ-ray irradiation was conducted by Soyagreentec (Hwaseong, Gyunggi-do, Korea) using a cobalt-60 irradiator (JS-10000, MDS-Nordion Inc., Kanata, ON, Canada) at 5, 10, 20, and 30 kGy. The irradiations were conducted at ambient temperatures. Non-irradiated controls were subjected to the same transport and storage conditions as the test samples.

2.4. Fracture force analysis

The mechanical fracture force of a single DMN was measured by a displacement force machine (Z0.5TN, Zwick/Roell Inc., Ulm, Germany) to confirm the effects of irradiation on the skin-penetrating function of a DMN patch. A single DMN was separated from the patch and attached to the stainless-steel station. The sensor probe pressed downwards vertically at a speed of 3.6 mm/min, and the axial force was recorded after the probe touched the DMN.

2.5. Microbial contamination and endotoxin contamination level tests

The microbial contamination test was conducted by the Korea Testing & Research Institute (KTR, Gwacheon, Gyunggi-do, Korea) on the basis of Korea Food and Drug Administration (KFDA) regulations of cosmetics (2014). The contamination levels were evaluated with 50.0 mL of distilled water containing six blister-packed DMN patches (approximately 1 g) homogeneously, measuring the total aerobic viable count for bacteria and total aerobic viable count for yeasts and molds, and detecting the presence of *Escherichia coli*, *Pseudomonas aeruginosa*, and *Staphylococcus aureus*.

Endotoxin levels were assessed using the limulus amebocyte lysate assay in sterile 96-well test plates. Blister-packed DMN arrays detached from a patch were dissolved in 1.0 mL of endotoxin-free reagent water, and each sample was diluted to a 1:10 ratio to compare simultaneously developed *Escherichia coli* O111:B4 endotoxin calibration curves, with concentrations ranging from 0.1 to 1.0 EU/mL ($R^2 \geq 0.98$). In addition, 2.0% (w/v) AA2G powder in 1 mL of endotoxin-free reagent water, 2.0% (w/v) HA powder in 1 mL of endotoxin-free reagent water and distilled water were also developed to measure endotoxin levels of individual product components. The absorbance was measured at a wavelength of 405 nm using a multimode plate reader (VICTOR™ X, PerkinElmer, Waltham, MA, USA).

2.6. Quantitative analysis of AA2G by HPLC

Reverse-phase HPLC using a C18 column (150 mm × 4.6 i.d., Cosmosil 5C18-AR-II, Nacalai Tesque Inc., Kyoto, Japan) and an HPLC system (Waters 600S, Waters, Milford, MA, USA) was performed to quantify AA2G. A stock solution of AA2G was serially diluted with distilled water to prepare the calibration curve, with concentrations ranging from 0 to 100 μg/mL ($R^2 \geq 0.99$). AA2G solution and AA2G-HA solution samples were also prepared in the range of the calibration curve. A solution containing HA only at a concentration of 500 μg/mL without AA2G was prepared as a negative control. In addition, DMN arrays of each patch in microtubes and blister packaging were detached from the sticky gel-foam sheet and dissolved in 1.0 mL of distilled water, to quantify the AA2G encapsulated in the DMN patch. Mobile phase A with a 0.1% (v/v) solution of TFA in distilled water and phase B with a 0.1% (v/v) solution of TFA in acetonitrile were used for the experiment. The phase A:B (99:1) remained isocratic, and the flow rate was 1.0 mL/min. The detection wavelength for AA2G was 254 nm.

2.7. Free-radical scavenging activity by DPPH assay

Free-radical scavenging activity of blister-packed DMN arrays was assessed using the DPPH assay in sterile 96-well test plates. DMN arrays detached from four patches were dissolved in 1.0 mL of distilled water, and 100-μL aliquots of the samples were added to each well. Next, 100 μL of 0.5-mM DPPH in ethanol was added to each sample, and the redox reaction was carried out at 25 °C for 20 min in a shaker (Changshin Scientific Co., Pocheon-si, Gyunggi-do, Korea). The absorbance of each sample was measured at a wavelength of 510 nm using a multimode plate reader. Radical scavenging activity was evaluated as follows:

Radical scavenging activity (%) = {1 − (absorbance of the samples/absorbance of the blanks)} × 100

2.8. In vitro permeation studies

In vitro permeation studies were conducted using a vertical-type Franz diffusion cell (Hanson, Chatsworth, CA, USA) with pig cadaver skin to confirm the effects of irradiation on release profile of AA2G of a DMN patch. DMN patches were applied using thumb force on skin and the tissues were mounted onto the donor compartment of the diffusion cell. The receptor chamber was filled with 7 mL of phosphate-buffered saline and maintained 32 °C using a water jacket. The studies were conducted using two groups of four cells composed of non-irradiated control group and e-beam-irradiated group at 40 kGy. With an occluded donor compartment, 1 mL of aliquots were withdrawn from the receptor compartment and the withdrawn was replaced by an equal volume of fresh phosphate-buffered saline at predetermined time points. The aliquots were analyzed using HPLC and the amount of lost due to phosphate-buffered saline replacement was calculated in the

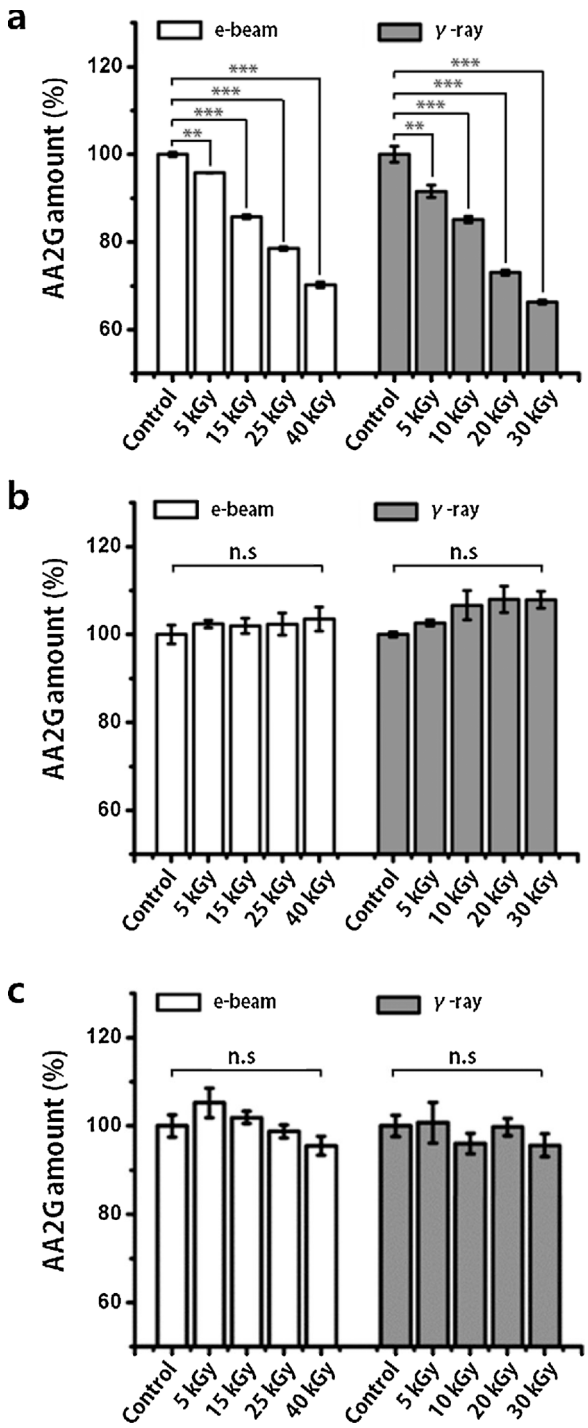

Fig. 6. Quantitative analysis of ascorbic acid 2-glucoside (AA2G) during the manufacturing process. (a) AA2G solution in microtubes showed a significant reduction in AA2G contents following both e-beam and γ-ray irradiation, indicating that AA2G in solution degrades easily. (b) AA2G-hyaluronic acid (HA) solution and (c) AA2G-HA dissolving microneedle (DMN) patches in microtubes maintained AA2G contents, which was expected because of the antioxidant activity of HA in both solution and solidified formulations (n = 4, mean ± SEM, $^{**}p < 0.01$, $^{***}p < 0.001$).

permeability graph.

2.9. Statistical analysis

SPSS (IBM, Armonk, NY, USA) was used for the statistical analysis. Comparisons of irradiation doses in e-beam and γ-ray group were analyzed by one-way analysis of variance (ANOVA) followed by a *post-hoc* Scheffe test, and comparisons between control group and e-beam-irradiated at 40 kGy group were analyzed by *t*-test. Statistical significance was set to $p < 0.05$, and values of $p < 0.05$, $p < 0.01$, and $p < 0.001$ were considered statistically significant.

3. Results and discussion

3.1. Preparation of AA2G-HA DMN patches

Fig. 1a illustrates the overall AA2G-HA DMN patch manufacturing process and packaging for terminal sterilization. The AA2G solution was mixed with HA powder to produce a viscous mixture of AA2G-HA solution, and this mixture was fabricated into AA2G-HA DMN patches. For packaging, two AA2G-HA DMN patches were placed in PET blisters pack and then sealed in aluminum foil wrappers, which are commonly used in DMN patch products. As shown in Fig. 1b, a single AA2G-HA DMN before terminal sterilization had an average length of 300.9 ± 4.5 μm, with an average tip diameter of 37.5 ± 0.96 μm (n = 4). The AA2G-HA DMN patch (7 × 7 microneedle array) was visualized (Fig. 1c) and placed in a PET blister pack (Fig. 1d), then sealed in a thick aluminum foil wrapper (Fig. 1e).

3.2. Morphology and fracture force analysis of AA2G-HA DMN patches

Since e-beam and γ-ray irradiation reduce the molecular weight of HA (Choi, Kim, Kim, Kweon, & Lee, 2010; Rehakova, Bakos, Soldan, & Vizarova, 1994), which is the backbone matrix of DMNs, irradiation sterilization may affect the morphology and strength of the DMNs. As shown in Fig. 2a, however, there were no visible morphological changes in the color and shape of the DMNs regardless of e-beam and γ-ray irradiation doses. This indicates that DMNs, which are composed of biopolymers, maintain their structure and are stable under radiation.

Although there were no visible morphological changes following e-beam and γ-ray sterilization, the fracture force, which is responsible for successful penetration of DMNs into the skin, could be altered; thus, analyzing the fracture force of DMNs after irradiation is important. As shown in Fig. 2b, the fracture of a single DMN, which was recorded along the axial of distance occurred as the peak of the graph (arrow). After irradiation (Fig. 2c), there were no significant differences in the fracture force between the control and the e-beam group (0.203 ± 0.014 N) or γ-ray group (0.185 ± 0.010 N) (n = 16, mean ± SEM). The fracture force was higher than 0.058 N, which is the minimum strength required for DMN skin penetration without fracture (Kim, Yang, Kim, Jung, & Jung, 2014). Because radiation sterilizations did not affect the physical properties of the AA2G-HA DMN patches, therefore, radiation that destroys microorganisms without heat, moisture, or chemicals would be suitable for DMN product sterilization.

3.3. Microbial contamination levels in AA2G-HA DMN patches

Microbial contamination levels were analyzed using terminal-sterilized AA2G-HA DMN patches in packaging for cosmetic use. Based on the KFDA guideline, total aerobic viable count for bacteria, yeast, and molds should be less than 500 CFU/mL, and *Escherichia coli*, *Pseudomonas aeruginosa*, and *Staphylococcus aureus* must not be detected in the samples. As shown in Table 1, the samples irradiated by e-beam and γ-ray met the limits of microbial contamination levels and contained levels similar to those of the control group. This implies that substances such as AA2G, HA, and distilled water were not contaminated by microorganisms, and there were no additional microbial contaminations during the overall AA2G-HA DMN patch manufacturing and packaging process.

3.4. Endotoxin contamination levels in AA2G-HA DMN patch

Based on the U.S. guidance for endotoxin testing, the endotoxin limit of medical devices for vaccination should be 20 EU per device (U.S. Food and Drug Administration, 2012). Therefore, terminal-sterilized AA2G-HA DMN patches in their packaging were also evaluated for endotoxin contamination. As shown in Fig. 3, both e-beam and γ-ray similarly reduced endotoxin levels in the DMN patches in a dose-dependent manner. On average, endotoxin levels were reduced under the limit by e-beam at 40 kGy and by γ-ray at 20 and 30 kGy. In particular, endotoxin levels in the AA2G-HA DMN patches were mainly attributable to HA powder, which contained 55.97 ± 7.05 EU per mg; AA2G and distilled water did not contain detectable endotoxin levels at the linear range of the calibration curve (n = 4, mean ± SEM). This indicates that the irradiations mainly reduced the endotoxins of HA in the DMN patches. Levels in the e-beam group decreased from 28.34 ± 3.02 EU (control) to 18.81 ± 2.02 (40 kGy) per patch, and in the γ-ray group, from 29.11 ± 1.66 EU (control) to 19.40 ± 3.52 EU (20 kGy) and to 18.20 ± 1.66 EU (30 kGy) per patch. This suggests that both e-beam and γ-ray affected endotoxin levels; however, the capacity to reduce endotoxin levels differed between the two irradiation methods: Higher irradiation doses were required for e-beam to decrease endotoxin levels effectively. Combined with the other findings, e-beam and γ-ray irradiation over 40 kGy and 20 kGy, respectively, satisfy the sterility requirements for both microbial and endotoxin contamination without loss of the DMN penetration function.

3.5. Quantitative analysis and free-radical scavenging activity of AA2G-HA DMN patches

Although the physical properties, such as morphology and fracture force, of AA2G-DMN patches were not affected by e-beam and γ-ray irradiation, satisfying the sterility requirements, we analyzed the effect of these irradiations on AA2G activity using HPLC quantitatively. As shown in Fig. 4a, γ-ray-irradiated samples at 10, 20, and 30 kGy showed significant decreases in AA2G quantities to 76.26 ± 1.24% ($p < 0.05$), 62.25 ± 5.07% ($p < 0.001$), and 53.46 ± 1.19% ($p < 0.001$), respectively. E-beam-irradiated samples showed no significant effects on AA2G content. This may be due to differences in penetration between e-beam and ɣ-ray. Since ɣ-ray penetrates more deeply at a lower dose into sterilizing materials than e-beam (Woo & Sandford, 2002), γ-ray could penetrate the packaging more easily than e-beam, degrading the encapsulated AA2G.

To confirm that the decrease in AA2G was related to a loss of AA2G activity, the free-radical scavenging activity, which forms the basis for the antioxidant properties of AA2G, was assessed. In parallel with quantitation analysis, the radical-scavenging activity only decreased following γ-ray irradiation; no significant differences were observed in the e-beam-irradiated group (Fig. 4b). In particular, the γ-ray group showed significant decrements at 20 kGy (1.74 ± 1.78%, $p < 0.05$) and 30 kGy (1.01 ± 1.84%, $p < 0.05$). This confirmed again that encapsulated AA2G degraded following γ-ray but not e-beam irradiation. Although γ-ray irradiation over 20 kGy satisfied the sterility requirement without loss of penetration function, this range of irradiation was not adequate for DMN sterilization due to the significant degradation of encapsulated AA2G. Therefore, only e-beam irradiation over 40 kGy, which satisfies the product sterility requirements without AA2G activity loss, should be considered suitable for terminal sterilization of DMNs.

3.6. Dissolution rate and in vitro permeation studies

Since terminal sterilization can affect dissolution rate and drug release of DMNs, non-irradiated group (control) and optimized e-beam-irradiated group at 40 kGy were compared in terms of decrease of the height of microneedle inside the skin and drug release profile of DMNs to epidermis. As shown in Fig. 5a, DMN structures of control group were gradually dissolved over time, which resulted in decrease of the height from 81.21 ± 6.71% at 5 min to 23.23 ± 5.63% at 20 min. In case of e-beam-irradiated group (40 kGy), there were no significant differences in dissolution rate compared with control group, which showed a decrease from 80.94 ± 7.68% at 5 min to 26.86 ± 2.10% at 20 min; this indicates that the dissolution rate was not affected by e-beam irradiation.

In permeation studies, both groups showed similar transdermal release profile over 24 h (Fig. 5b). In particular, delivery of AA2G was increased and saturated over 12 h and completely delivered at 24 h (control; 97.65 ± 21.60%, e-beam at 40 kGy; 102.35 ± 17.42%). Since there were no significant differences between two groups at each time points, this result, in parallel with dissolution rate analysis, confirmed that e-beam irradiation did not affect release profile of AA2G.

3.7. Quantitative analysis of AA2G during each step of the manufacturing process and the effect of HA

Although terminal sterilization is the process whereby a product is sterilized in its final packaging, in-depth analysis of the effects on AA2G activity is required, since AA2G interacts with HA in different states during the DMN fabrication and packaging process. Thus, we analyzed the effect of the irradiations on AA2G activity following each step of the manufacturing process. AA2G solution, AA2G-HA solution, and AA2G-HA DMN patches were analyzed using HPLC and irradiated in microtubes. As shown in Fig. 6a, AA2G solution displayed a statistically significant decrease in AA2G content following both e-beam and ɣ-ray irradiation at all doses, which indicates that AA2G in solution could be easily degraded by irradiation. The total reduction in AA2G content in the ɣ-ray-irradiated group was higher than the reduction in the e-beam group. AA2G content decreased from 91.57 ± 1.43% (5 kGy, $p < 0.01$) to 66.32 ± 0.46% (30 kGy, $p < 0.001$) following ɣ-ray irradiation, whereas the e-beam irradiations resulted in less reduction, even at 40 kGy, from 95.80 ± 0.08% (5 kGy, $p < 0.01$) to 70.20 ± 0.66% (40 kGy, $p < 0.001$). This finding confirmed again that the γ-ray penetrated the microtubes more easily than the e-beam, and that ɣ-ray irradiation degraded AA2G at a higher rate than e-beam irradiation.

Adding HA to the AA2G solution prevented reductions in AA2G content by irradiation (Fig. 6b), whereas AA2G in solution degraded readily. This indicates that HA can protect AA2G from degrading even in a dissolved state. Since irradiating HA with e-beam or ɣ-ray could improve the reducing power or radical-scavenging activity of HA itself, as other studies have suggested (Choi et al., 2010; Kim et al., 2008), it is expected that irradiated HA in solution could react with radicals generated by the irradiation, thereby protecting the encapsulated AA2G. Moreover, the reactivity of HA with radicals is expected to be higher than that of AA2G. In many cases, antioxidants can be added to polymer solutions to reduce the effects of irradiation on the mechanical properties or physical appearance of the polymer (Ghani et al., 2014; Hawkins, 1984; International Atomic Energy Agency, 1999). In contrast, HA played an antioxidant role in AA2G-HA solution and stabilized the quantity of AA2G capable of antioxidant activity. From these perspectives, HA added to AA2G solution could be used as a biodegradable backbone polymer capable of skin penetration, and also as a stabilizer to protect the encapsulated drug during irradiation in the terminal-sterilization process.

We found no significant differences in AA2G contents between control and irradiated samples of AA2G-HA DMN patches (Fig. 6c). This confirmed again that AA2G could be protected from degradation by the presence of HA at a solidified formulation of the AA2G-HA solution. Moreover, the results of irradiating AA2G-HA DMN patches by ɣ-ray in packaging (Fig. 4a) and in microtubes (Fig. 6c) clearly indicate the effect of the irradiation on packing materials. AA2G contents in the packaging group decreased markedly, but were preserved in the

microtubes; this implies that γ-ray irradiation penetrated the final packaging material (PET blister pack and aluminum foil wrapper) more easily than the microtubes, and the radiation penetrated the packaging degraded the encapsulated AA2G despite the antioxidant activity of HA.

4. Conclusions

In this study, we introduced a detailed analysis of terminal sterilization of HA-based DMN patches for meeting product sterility requirements without activity loss of the encapsulated drugs. We found that neither e-beam nor γ-ray irradiation affected the physical properties of DMNs, and could effectively reduce microorganismal and endotoxin contamination levels. However, γ-ray doses satisfying the sterility requirement (20 and 30 kGy) also degraded the encapsulated drug, whereas e-beam irradiation (40 kGy) maintained the quantity and activity of the drug without affecting the dissolution rate and release profile in its final packaging. Thus, e-beam, which provides lower penetration and higher doses into sterilizing materials, is suitable for terminal sterilization of DMNs; this approach can advance developments in transdermal drug delivery.

Acknowledgements

This work was supported by the R & D program of MSIP/COMPA (2016K000225, Development of minimal pain multi-micro lancets for one-touch-smart diagnostic sensor) and by a grant from the Korea Health Technology R & D Project through the Korea Health Industry Development Institute (KHIDI), funded by the Ministry of Health & Welfare, Republic of Korea (grant number: HI14C0365); the work was also partially supported by the Graduate School of Yonsei University Research Scholarship Grants in 2017.

References

Ameri, M., Wang, X., & Maa, Y. F. (2010). Effect of irradiation on parathyroid hormone PTH(1-34) coated on a novel transdermal microprojection delivery system to produce a sterile product-adhesive compatibility. *Journal of Pharmaceutical Sciences, 99*, 2123–2134.

Anirudhan, T. S., Nair, S. S., & Nair, A. S. (2016). Fabrication of a bioadhesive transdermal device from chitosan and hyaluronic acid for the controlled release of lidocaine. *Carbohydrate Polymers, 152*, 687–698.

Asasutjarit, R., Theerachayanan, T., Kewsuwan, P., Veeranondha, S., Fuongfuchat, A., & Ritthidej, G. C. (2017). Gamma sterilization of diclofenac sodium loaded-*N*-trimethyl chitosan nanoparticles for ophthalmic use. *Carbohydrate Polymers, 157*, 603–612.

Becker, L. C., Bergfeld, W. F., Belsito, D. V., Klaassen, C. D., Marks, J. G., Jr., Shank, R. C., et al. (2009). Final report of the safety assessment of hyaluronic acid, potassium hyaluronate, and sodium hyaluronate. *International Journal of Toxicology, 28*(Suppl. 4), 5–67.

Chandrasekharan, D. K., Kagiya, T. V., & Nair, C. K. K. (2009). Radiation protection by 6-palmitoyl ascorbic acid-2-glucoside: Studies on DNA damage in vitro, ex vivo, in vivo and oxidative stress in vivo. *Journal of Radiation Research, 50*, 203–212.

Choi, J. I., Kim, J. K., Kim, J. H., Kweon, D. K., & Lee, J. W. (2010). Degradation of hyaluronic acid powder by electron beam irradiation, gamma ray irradiation, microwave irradiation and thermal treatment: A comparative study. *Carbohydrate Polymers, 79*, 1080–1085.

Chu, L. Y., Choi, S. O., & Prausnitz, M. R. (2010). Fabrication of dissolving polymer microneedles for controlled drug encapsulation and delivery: Bubble and pedestal microneedle designs. *Journal of Pharmaceutical Sciences, 99*, 4228–4238.

Ghani, M. H. A., Salleh, M. N., Chen, R. S., Ahmad, S., Hamid, M. R. Y., Hanafi, I., et al. (2014). The effects of antioxidants content on mechanical properties and water absorption behaviours of biocomposites prepared by single screw extrusion process. *Journal of Polymers, 2014*, 1–6. http://dx.doi.org/10.1144/2014/243078.

Girennavar, B., Jayaprakasha, G. K., Mclin, S. E., Maxim, J., Yoo, K. S., & Patil, B. S. (2008). Influence of electron-beam irradiation on bioactive compounds in grapefruits (*Citrus paradisi* Macf.). *Journal of Agricultural and Food Chemistry, 56*, 10941–10946.

Giudice, E. L., & Campbell, J. D. (2006). Needle-free vaccine delivery. *Advanced Drug Delivery Review, 58*, 68–89.

Grieb, T., Forng, R. Y., Brown, R., Owolabi, T., Maddox, E., McBain, A., et al. (2002). Effective use of gamma irradiation for pathogen inactivation of monoclonal antibody preparations. *Biologicals, 30*, 207–216.

Hawkins, W. L. (1984). Polymer degradation and stabilization. In H. J. Harwood (Ed.). *Polymer – Properties and applications 8* (pp. 74–90). Berlin: Springer-Verlag Berlin Heidelberg Co.

International Atomic Energy Agency (1999). *Stability and stabilization of polymers under irradiation. Final report of a co-ordinated research project, 1994–1997* Accessed at http://www-pub.iaea.org/MTCD/Publications/PDF/te_1062_prn.pdf on June 11, 2017.

Kim, J. K., Srinivasan, P., Kim, J. H., Choi, J. I., Park, H. J., Byun, M. W., et al. (2008). Structural and antioxidant properties of gamma irradiated hyaluronic acid. *Food Chemistry, 109*, 763–770.

Kim, Y.-C., Park, J.-H., & Prausnitz, M. R. (2012). Microneedles for drug and vaccine delivery. *Advanced Drug Delivery Review, 64*, 1547–1568.

Kim, J. D., Kim, M., Yang, H., Lee, K., & Jung, H. (2013). Droplet-born air blowing: Novel dissolving microneedle fabricationDroplet-born air blowing: novel dissolving microneedle fabrication. *Journal of Controlled Release, 170*, 430–436.

Kim, M., Yang, H., Kim, H., Jung, H., & Jung, H. (2014). Novel cosmetic patches for wrinkle improvement: Retinyl retinoate- and ascorbic acid-loaded dissolving microneedles. *International Journal of Cosmetic Science, 36*, 207–212.

Kim, S., Yang, H., Kim, M., Baek, J. H., Kim, S. J., An, S. M., et al. (2016). 4-n-butylresorcinol dissolving microneedle patch for skin depigmentation: A randomized, double-blind, placebo-controlled trial. *Journal of Cosmetic Dermatology, 15*, 16–23.

Kong, M., & Park, H. J. (2011). Stability investigation of hyaluronic acid based nanoemulsion and its potential as transdermal carrier. *Carbohydrate Polymers, 83*, 1303–1310.

Kong, B. J., Kim, A., & Park, S. N. (2016). Properties and *in vitro* drug release of hyaluronic acid-hydroxyethyl cellulose hydrogels for transdermal delivery of isoliquiritigenin. *Carbohydrate Polymers, 147*, 473–481.

Korea Food and Drug Administration (2014). *Regulations on the safety standards, etc. of cosmetics, Notification no. 2014-118.* Cosmetics Policy Division.

Marreco, P. R., da Luz Moreira, P., Genari, S. C., & Moraes, A. M. (2004). Effects of different sterilization methods on the morphology, mechanical properties, and cytotoxicity of chitosan membranes used as wound dressings. *Journal of Biomedical Materials Research. Part B, Applied Biomaterials, 71B*, 268–277.

Mathew, D., Nair, C. K. K., Jacob, J. A., Biswas, N., Mukherjee, T., Kappor, S., et al. (2007). Ascorbic acid monoglucoside as antioxidant and radioprotector. *Journal of Radiation Research, 48*, 369–376.

Mistilis, M. J., Bommarius, A. S., & Prausnitz, M. R. (2015). Development of a thermostable microneedle patch for influenza vaccination. *Journal of Pharmaceutical Sciences, 104*, 740–749.

Park, J.-H., Allen, M. G., & Prausnitz, M. R. (2005). Biodegradable polymer microneedles: Fabrication, mechanics and transdermal drug delivery. *Journal of Controlled Release, 104*, 51–66.

Prausnitz, M. R., & Langer, R. (2008). Transdermal drug delivery. *Nature Biotechnology, 26*, 1261–1268.

Rehakova, M., Bakos, D., Soldan, M., & Vizarova, K. (1994). Depolymerization reactions of hyaluronic acid in solution. *International Journal of Biological Macromolecules, 16*, 121–124.

Rogers, J. (2010). Venous thromboprophylaxis: Reducing needlestick injury. *Nursing Standard, 24*, 35–41.

Rowland, M. (1972). Influence of route of administration on drug availability. *Journal of Pharmaceutical Science, 61*, 70–74.

Silindir, M., & Ozer, A. Y. (2009). Sterilization methods and the comparison of e-beam sterilization with gamma radiation sterilization. *FABAD Journal of Pharmaceutical Sciences, 34*, 43–53.

Singh, R., Singh, S., & Lillard, J. W. (2008). Past, present and future technologies for oral delivery of therapeutic proteins. *Journal of Pharmaceutical Science, 97*, 2497–2523.

Tadwee, I. K., Gore, S., & Giradkar, P. (2011). Advances in topical drug delivery system: A review. *International Journal of Pharmaceutical Research & Allied Science, 1*, 14–23.

Tidswell, E. C. (2011). Sterility. In M. R. Saghee, T. Sandle, & E. C. Tidswell (Eds.). *Microbiology and sterility assurance in pharmaceuticals and medical devices (2011th ed.)* (pp. 589–614). New Delhi: Business Horizons.

U.S. Food & Drug Administration (2004). *Guidance for industry: Sterile drug products produced by aseptic processing – Current good manufacturing practice.* U.S. Department of Health and Human Services September 2004.

U.S. Food & Drug Administration (2012). *Guidance for industry: Pyrogen and endotoxins testing: Questions and answers.* U.S. Department of Health and Human Services.

Wong, P. Y. Y., & Kitts, D. D. (2001). Factors influencing ultraviolet and electron beam irradiation-induced free radical damage of ascorbic acid. *Food Chemistry, 74*, 75–84.

Woo, L., & Sandford, C. L. (2002). Comparison of electron beam irradiation with gamma processing for medical packaging materials. *Radiation Physics and Chemistry, 63*, 845–850.

Yang, H., Kim, S., Kang, G., Lahiji, S. F., Jang, M., Kim, Y. M., et al. (2017). Centrifugal lithography: Self-shaping of polymer microstructures encapsulating biopharmaceutics by centrifuging polymer drops. *Advanced Healthcare Materials, 2017*, 1700326. http://dx.doi.org/10.1002/adhm.201700326.